AIR ENTRAINMENT IN DIP COATING UNDER REDUCED AIR PRESSURES

H. Benkreira[1] and M.I.Khan

School of Engineering, Design & Technology
University of Bradford, United Kingdom

ABSTRACT

This study examines experimentally and for the first time the effect of reduced air pressure on dynamic wetting. The purpose is to assess the role of air viscosity on dynamic wetting failure which hitherto has been speculated on but not measured. In this paper we used dip coating as the model experimental flow and report data on air entrainment velocity V_{ae} we measured with a series of silicone oils in a range of viscosities in a vacuum chamber where the pressure can be reduced from atmospheric down to a few mbar when the mean molecular free path of air is large and air ceases to have a viscosity. To complement earlier work, we carried out the experiments with a range of substrates of varying roughness. The substrates were chosen so that for each one, their two sides differ in roughness. This enables simultaneous comparative observation of their wetting performance and reduces the experimental error in assessing the role of roughness. The data presented here capture the effects of viscosity, roughness and air pressure but the important result of this study is that V_{ae} can be increased considerably (exponentially) when the pressure is reduced with the suggestion that V_{ae} approaches infinity as pressure approaches zero. In other words, the role of the surrounding air viscosity is important in dynamic wetting. The data from this study have significant implication to the fundamental understanding of dynamic wetting. Indeed they form the missing data link to fully understand this phenomenon. The data presented in this work also confirm the complex role of roughness, in that it can increase or decrease the air entrainment speed depending on the value on the viscosity of the coating solution. The results presented in this paper are very useful in practice as they imply that if one chooses carefully roughness one can coat viscous formulation at unexpectedly very high speeds with a moderate vacuum (50 mbar typically).

Keywords : *Dip Coating; Coating flows; Air entrainment; Dynamic wetting; - Contact angle; Experiments; Air viscosity (vacuum pressure)*

1. INTRODUCTION

Dynamic wetting is the process by which air or another gas on and around a solid surface is displaced by a liquid and its simplest experimental representation is the

[1] corresponding author : Tel (01274) 383721 Fax (01274) 385700 Email H.Benkreira@bradford.ac.uk

steady dipping of a solid web into a pool of liquid. Dynamic wetting occurs in many flow situations but most typically in all coating flows which must all *begin* with a dynamic wetting line which, as shown in Fig. 1, forms with the moving solid surface (substrate) a dynamic contact angle θ_D. Ablett (1923) was the first to report from his dip coating experiments that this contact angle increased steadily with the speed of the substrate and to approach a maximum value of 180° at which point the displaced air begins to be entrained between the solid and the displacing liquid and *dynamic wetting failure* can be said to occur. In the practical context of coating operations, air entrainment is wholly undesirable as it limits processing speeds, hence productivity and if unnoticed will lead to defective unsaleable films. Clearly, understanding this phenomenon and perhaps postponing its occurrence to higher speeds by manipulating the flow and substrate conditions is of huge industrial interest. Deryagin and Levi (1964) were the first to reveal experimentally how dynamic failure occurred: the dynamic wetting line which is originally straight, suddenly breaks up and adopts a sawtooth shape; the flow becomes unstable and three-dimensional and air is entrained at the trailing vertices where two straight-line segments of the wetting line seem to intersect (Fig. 1). Several studies then followed to correlate the critical speed V_{ae} at which dynamic wetting failure occurs with the physical properties of the coating liquid. All the studies agree that the coating liquid viscosity is the key parameter with surface tension playing a secondary role only. The most often quoted experimental correlation is that due to Gutoff and Kendrick (1982):

$$V_{ae} \approx 5.11\,\mu^{-0.67} \qquad [1]$$

where V_{ae} is expressed in m/s and μ in mPa.s. This correlation is applicable only with Newtonian fluids. Non-Newtonian effects on wetting are more complicated and have not been fully resolved. Cohu and Benkreira (1998) reported that in the case of non-Newtonian solutions made up of polymers dissolved in a solvent, air entrainment speeds computed with the viscosity of the pure solvent were a good approximation to those they measured with the polymer solutions. These results suggest that the dynamic wetting failure velocity is determined by interactions of the smaller molecules near the contact line and not by the the polymer macromolecules and the bulk rheology of. coating fluid.

Perhaps the most fundamental explanation of dynamic wetting is that given by Blake and Ruschak (1979) who measured the angle Φ of the sawteeth shaped wetting line (see Fig.1) at speeds higher than V_{ae} and observed that the product $V_{ae} \cos \Phi$ remained constant thus establishing that the component of the speed normal to the straight-line segments of the wetting line was independent of the substrate velocity. They termed this component, the *maximum speed of wetting*, V* which they assumed is the maximum speed at which the wetting line can advance normal to itself. They then proposed the following mechanism of air entrainment in coating flows. When the velocity of the substrate exceeds V*, the wetting line adopts a sawtooth shape so that the component of the speed of the solid normal to the segments of the wetting line does not exceed V*. This enables the lengthened wetting lines to continue to wet the solid. However, the curvature of the wetting line is large but finite at the point where two of its straight-line segments seem to intersect, so that the tangent to the wetting line at this point remains normal to the velocity of the solid. This point of the wetting line is then drawn into the liquid since its speed relative to the substrate cannot exceed

V*. This explains why air is entrained only at the trailing vertices where two straight-line segments of the wetting line seem to intersect. Seen like this, air entrainment appears as a *consequence* of the break-up of the wetting line which occurs because the speed of the wetting line normal to itself is restricted. Expressed mathematically, at speeds V equal or higher than V*, the wetting line segments adopt the minimum possible inclination Φ such that:

$$\cos \Phi = V^*/ V \qquad (V \geq V^*) \qquad [2]$$

Cohu and Benkreira (1998) observed that a corollary to this equation is that air entrainment could be postponed to velocities V_{ae} greater than V* in coating flows where the wetting line is not perpendicular but tilted at an angle β to the direction of substrate motion. They tested this corollary in their angled dip coating (Cohu and Benkreira, 1998) and angled die coating (Benkreira and Cohu, 1998) experiments at various angles β with a range of different viscosities and surface tensions coating liquids and found the corollary to hold true and that:

$$V_{ae} = V^* /\cos \beta \qquad [3]$$

where V* is the air entrainment velocity at β=0 . Put in numbers, this corollary states that air entrainment speed can be doubled by tilting the angle of entry β from 0 to 60^0.

Another corollary to the concept of the maxiumum speed of wetting is that roughness should decrease V_{ae} on the basis that the wetting line must move a greater distance across a rough surface than a flat surface of equivalent length. This contradicts the hydrodynamic proposition made by Scriven (1982) that with rough surfaces, air can escape through the valleys between peaks in the surface. The data of Buonopane *et al.* (1986) suggests that this is the case with roughness increasing V_{ae} in some cases by a factor as much as 12 in comparison with smooth substrates. Recently, Benkreira (2004) carried out experiments with substrates that were smooth on one side and rough on their other side and established that roughness could increase or decrease V_{ae} depending on the value of the viscosity of the coating fluid. In particular, he observed that a rough substrate will only coat faster than a smooth substrate when the viscosity exceeds a critical value. The higher the roughness, the larger the critical viscosity will be. In other words, at a given viscosity, normally a smooth surface coats faster than a rough surface but beyond a critical viscosity a "switch" or the reverse is observed. The data showed that the rougher the surface, the larger the critical viscosity will be. This observation is very useful in practice as it implies that if one chooses carefully roughness one can coat viscous formulation at unexpectedly very high speeds. These results suggest that air entrainment may not be just a molecular scale event as inferred by Blake and Rushack (1979) and that hydrodynamic effects play an important role.

Clearly, despite all the progress made in understanding dynamic wetting failure and the established fact that the formation of these triangular structures at the contact line is a prerequisite for air entrainment, we still do not have an accepted full proof theory of dynamic wetting. We still do not know *why the triangular structure forms and what is their physical origin and the physical origin of the assumed maximum speed of wetting.* Also, the difficulties of resolving our observations of dynamic wetting at the very small scale makes it difficult to measure accurately the

dynamic contact angle and assess how and with what it changes. These difficulties divide the type of theories that may be devised to explain this important phenomenon. Existing theories of dynamic wetting that can fit available experimental data broadly divide into two groups. The first group (Blake and Haynes, 1969; Blake, 1993 ; Shikhmurzaev, 1993, 1997) considers events occuring at the molecular scale at the dynamic wetting line and require very careful observations of the dynamic wetting region. They predict the existence of a maximum speed of wetting even if the displaced phase (*i.e.* air) is inviscid. In other words, air is not *responsible* for the break-up of the wetting line that ultimately causes air entrainment as explained above. On the other hand, the second group of theories (Teletzke *et al*., 1988; Miyamoto, 1991 and references therein) consider events at macroscopic scale - the hydrodynamics of the air-liquid system. In other words, these theories consider air viscosity to be important. Being a viscous fluid, air is assumed to be always entrained as an invisible film due to the viscous drag arising from the movement of the surfaces of both the liquid and solid. As the substrate speed increases, the air film thickens, leading to visible air entrainment. Although such a model of dynamic wetting do not actually predict the break-up of the wetting line into a sawteeth pattern, the experiments of Veverka and Aidun (1997) suggest that the formation of triangular air pockets could be due to interfacial instability of the liquid surface adjacent to the entrained flat layer of air. Interestingly, the hydrodynamic model of dynamic wetting predict the existence of a maximum speed of wetting only when the viscosity of the displaced phase is non zero (Cox, 1986).

It is also interesting to note that the hydrodynamic model seems to apply better when the displaced phase is a viscous liquid instead of air. Indeed, whilst the appearence of sawtooth-shaped wetting lines at an air/liquid/solid interface is widely documented in the literature (*e.g.* Deryagin and Levi, 1959; Wilkinson, 1975; Burley and Kennedy, 1976; Blake and Ruschak, 1979; O'Connell, 1989; Cohu and Benkreira, 1998), no similar observations have been reported for situations where the displaced phase is a viscous liquid. This suggests that the phenomenon of dynamic wetting failure does not relate with the fact that air has a viscosity but may be somewhat hindered by the hydrodynamic entrainment of the displaced phase when the latter is viscous. In order to provide experimental evidence of this hypothesis, dynamic wetting experiments in the absence of surrounding air or gas are required. This is precisely the subject of this paper which reports an experimental study of the dynamic wetting of a solid substrate by a liquid under high vacuum pressures down to 1 mbar. Under these pressures, the mean molecular free path of air is large[2] and about 66 μm, of order similar or larger than the thickness of the air film inside the triangular pockets (measured under atmospheric pressure to be 10 to 30 μm by Severtson and Aidun. 1996), the air molecules rarely run into each other and air ceases to have a viscosity. Under such conditions, the presence of the triangular structures at the dynamic wetting line would give evidence in favour of molecular theories, especially if the critical speeds are found to be independent on whether air is present or not. Conversely, the absence of such structures would prove the active role of air and hydrodynamics in their formation.

2. EXPERIMENTAL METHOD

[2]For air at 300K, the mean free path in mm =6.6/P with P in Pa.

The Apparatus: The experimental apparatus is depicted schematically in Fig. 2 and consists essentially of a 50 mm wide tape drawn downwards through a perpex tank containing the liquid. The dimensions of the tank were 150 × 135 × 90 mm (height, h, × depth, 2d, × width, w). The tape passed over grounded metal rollers to reduce any static charges, plunged into the liquid, emerged from a narrow slit at the bottom of the tank and was finally wound around a cylinder driven by a variable speed motor. This simple design prevented the fluid carried along the substrate at exit of the pool from flowing back and entraining air bubbles into the tank. Another advantage was that the bulk flow of the liquid within the tank on either side of the tape far from its edges is a well-defined free-surface side-driven cavity flow. The aspect ratio a_c of the liquid pool is defined as the tape-to-wall distance, d, divided by the liquid height, H (that is a_c=d/H). Although the liquid height H was allowed to change during the experiments, as some liquid was entrained out of the pool by the substrate, the aspect ratio was always kept between 0.6 and 1.6, and it was checked that the results were insensitive to changes in a_c within this range. In all cases, additional liquid was supplied regularly to the tank to compensate for the amount entrained out of the pool by the substrate.

The Vacuum Chamber: The dip coater system, including the tank and the motor, was designed to be compact, the inter-axes distance between the feed reel and the take-up reel being approximately 55 cm. The whole set-up, excluding the motor, was housed in a 1cm thick wall, vacuum steel welded chamber (80 cm x 40 cm x 40 cm). The chamber had a removable access door and three laminated glass viewing windows around the dynamic wetting region. The non-welded parts were sealed with O-rings and rubber sleeves and the whole closed chamber was tested for leaks prior to the experiments (further details below on the measurement of pressures). To prevent overheating, the substrate winder roller was driven from the outside by a geared motor via a labyrinth type vacuum seal. The substrate speed was measured by a remote sensor suitably calibrated and placed inside the vacuum chamber. A high vacuum pump (BOC Edwards E2M 12, 2 Stage) was used to create the required pressures in the chamber. Before the air entrainment experiment could be carried out, the vacuum pump was switch on and left for as long as it took to degas the solution tested and this degassing time depends on the viscosity of the solution. Typically with a 20 mPa.s silicone oil, a vacuum of less than 10 mbar was achieved in 90 minutes whereas with the 200 mPa.s it took as long as 3 hours to obtain a vacuum down to 40 mbar. Once the required vacuum was reached, the pump was switched off, then a needle valve was used to bleed-off some of the vacuum and we could begin the air entrainment experiments from a set minimum pressure. Subsequent experiments were carried out by further bleeding through the needle valve. Two vacuum gauges, suitably calibrated, were mounted to monitor the pressure inside the chamber, one with a large range 1 down to 0 bar and a second with a smaller range 50 to 0 mbar. The temperature of the coating fluid and the air inside the chamber was monitored throughout the experiments.

The Coating Fluids: In order to avoid evaporation of the coating liquids at the low vacuum pressures, we used a number (6) of silicone oils (Basildon Chemicals) of partial pressures << 1mbar and in a viscosity range 10 to 500 mPa.s and surface tension 18.5-20.0 mN/m. Glycerine-water solutions (9) with viscosities ranging from 40 to 733 mPa.s and surface tension 65 mN/m were also used in the experiments at

atmospheric pressure. The glycerine-water solutions were mixed at low speed for 24 hours with a propeller mixer and left to rest overnight prior to the coating experiments. With this standardized method of preparation, uncertainties resulting from undesirable effects such as absorption of air moisture by glycerin could be minimized. The physical properties of the liquids were measured at the temperature recorded during the coating experiments, which did not vary significantly during the processing of each individual liquid. All the experiments were conducted at room temperature, that is between 20 and 25 °C. The viscosity of the fluids were measured to an accuracy of ± 5% in a Bohlin CVO viscometer equipped with a Peltier system allowing an accurate control (within 0.1 °C) of the sample temperature. The viscosity was measured over a range of shear rates and temperatures and were found to be Newtonian as expected. The surface tensions of the fluids were measured to an accuracy of ± 2 % with a FTA 188 video tensiometer using the pendent drop method.. The surface tensions were also measured at T_{exp} ± 0.1 °C. For each liquid, air entrainment experiments, rheological characterizations, and whenever possible surface tension measurements were carried out on the same day to minimize errors due to air-moisture absorption or bio-degradation. The physical properties of all the coating fluids tested are shown in Table 1 at typical tested temperatures.

The Substrates: In order to assess the relative effect of surface roughness on air entrainment under low pressures, we used 2 non porous coated papers (Pap) and 3 polyester (Plast) substrates. By design and unique to this programme of research, each of these substrates had different front and back roughness. Their labelling thus was Pap1F, Pap1B, Pap2F, Pap2B, etc. and Plast1F, Plast2B, etc. The sourcing of substrates with dual roughness is very useful as one experiment under identical conditions enables the simultaneous viewing of both sides of the substrate and assess accurately the relative effect of roughness (see Benkreira, 2004). The topography of the substrates was characterized using three instruments: a Taylor Hobson series Talysurf 4, a comparatively crude roughness measurement device, a surface-mapping microscope, a more comprehensive 3D profiling of the surface and an PicoForce Multimode Atomic Force Microscope which can zoom on roughness at a very small scale of scrutiny. All three devices were used in order to distinguish between those substrate sides that were similar in roughness. Remember that many lengths can be used to define roughness including peak height, valley depth, the sum of the two, their arithmetic average, maximum, root mean square and other indices. Table 2 gives the the average peak-to-valley height roughness R_z measured using the Talysurf method and is a comprehensive basis for ranking the substrates. Note that with each instrument and with each sample, the measurements were repeated at least 5 times. The data in Table 2 show that the two paper substrates have distinct roughness on their sides with R_z varying from 0.70 to 4.40 μm. The 3 polyester substrates have on the other hand much lower roughness ranging in R_z from 0.19 to 1.92 μm. If we assume that $R_z < 1$ μm and $R_z > 1$ μm distinguishes between smooth and rough substrates, we have thus a full combination to assess from, i.e. distinguish between the rough and the smooth and various levels of roughness. It is important to note that *a-priori* these experiments can only distinguish the effect of roughness for a given material, i.e we should not expect that for equal roughness, a paper surface will exhibit the same V_{ae} as a polyester substrate. Our experiments with these two very different materials (and the two materials mostly used as substrates in the coating industry) are therefore very useful in assessing this effect.

Now, another method of characterising the substrates - that of measuring the dynamic contact angle of a drop of the fluid tested on the substrate utilised - was used in this study. This method captures topographic effect as well as material effect. In fact, it is a measure of the surface energy of these substrates. We used for this purpose an FTA 188 video tensiometer which delivers a drop onto a surface and via camera connected to a computer enables to track the change of the contact angle with time until it reaches its equilibrium value. Table 2 gives values of the contact angle at t = 0 s and t = 3 s for the substrates tested to highlight this characteristic. Figure 3 gives the complete variation in time of the contact angle for the various liquid-substrate system tested in the coating trials.This surface energy technique is particularly discerning when effects other than roughness are sought and is useful for assessing substrates of similar roughness or similar equilibrium contact angle.

The Measurement of V_{ae}: The air entrainment speed was measured by illuminating the wetting line area through the chamber windows, increasing slowly the substrate speed and measuring either the speed at which the dynamic wetting line breaks into "vvv" segments if these appeared or the speed at which we could see air bubbles being entrained in the flow. Remember that under atmospheric conditions, we know that when the dynamic wetting line breaks into "vvv" segments, air bubbles form at the tip of the segment and are entrained into the liquid. The observations were carried out visually when large "vvv" were formed or with the aid of a colour CCD camera with magnification up to 33 times and a long distance microscope linked to an image display-recording system. In order to reduce experimental errors, each data point was repeated at least five times. The relative standard deviation was always found to be lower than 3.5%, being even less than 2% in most cases. All coating experiments were conducted at room temperature (between 20 and 27 °C), and the actual temperature of the liquid, T_{exp}, was carefully recorded, for the purpose of measuring the physical properties of the coating liquid.

Further details on the experimental method as well as a presentation of all data pertaining to this study can be found in Khan (2006).

3. RESULTS AND DISCUSSION

3.1. Validation of the Experimental Technique

In order to validate the experimental technique, V_{ae} was measured at atmospheric pressure using the smooth polyester substrates and glycerine-water solutions. These are the conditions used by most previous researchers including Burley and Kennedy (1976), Gutoff and Kendrick (1982), Burley and Jolly (1984), Cohu and Benkreira (1998) and Blake and Shikhmurzaev (2002). The comparisons between our measured V_{ae} and those measured by these workers are presented in Fig. 4. There is a good agreement between all the data but particularly very good agreement with the data of Cohu and Benkreira (1998) and Blake and Shikhmurzaev (2002) who all used photographic type support substrates similar to ours. Figure 4 also includes the experimental correlation of Gutoff and Kendrick's (1982) obtained with a series of fluids. The very good agreement confirms the primary effect of viscosity on air entrainment speeds. Figure 4 shows also V_{ae} we measured on the same substrates with silicone oils which have a much lower surface tensions (20 as against 65 mN/m for glycerine solutions). In comparison, V_{ae} measured with silicone oils is lower than

that measured with glycerol solutions, particularly at lower viscosities. The same observation on the effect of surface tension has been made by Burley and Kennedy (1976), Burley and Jolly (1984) and Cohu and Benkreira (1998) and confirm the accuracy of our experimental technique.

3.2 Effect of Vacuum Pressures on Smooth Substrates

Here the substrates considered are one side of one paper (Pap1B) and both sides of the two polyester Plast2 and Plast3 or 5 substrates altogether all of roughness R_z<1 μm as indicated in Table 2. These substrates were tested over a range of silicone oils viscosities and the observations were as follows.

- In all cases and with all the pressures tested down to 20 mbar, dynamic wetting failure manifested itself with the appearance of the "vvv line". In other words the nature of the dynamic wetting failure remains the same as we decrease pressure.
- Typically, with our substrate of 60 mm width, there were about 10 "v" at atmospheric pressure with the 200 mPa.s viscosity silicone oil. With the 20 mPa.s, there were only 2 "v" at atmospheric conditions. Similar observations have been reported at atmospheric conditions by Burley (1992). Figure 5 shows 1 large "v" extending some 5 cm from the liquid surface all the way through the rubber slit at the bottom of the tank with the glycerol solution of viscosity 40 mPa.s at atmospheric pressure.
- Generally, the size of the "v" decreased and their number increased (becoming smaller and difficult to see) with decreasing pressure at a constant viscosity. Clearly, when the pressure is reduced drastically away from atmospheric, the propensity of the substrate to entrain air is being diminished.
- With all the four silicone oils and the two smooth polyester substrates tested, the air entrainment speeds measured at constant viscosity were found to be almost identical (+/-3.5%) on both sides of these substrates. Figure 6a gives data for Plast2F/B for four viscosity values. In order not to cluter Fig. 6a, only Plast3F is added to the figure which shows clearly the polyester substrate performing almost identically front and back over the range of viscosities and pressures tested. These results in the measured V_{ae} reinforce the accuracy of our technique since these substrates are smooth on both sides.
- The air entrainment data presented in Fig. 6a show that at constant viscosity, V_{ae} does not vary very much when the air pressure was reduced from 1 bar to 500 mbar but a sharp increase was measured at pressures below 200 mbar with more than a doubling of V_{ae} when the pressure is reduced to 20 mbar. Typically the air entrainment speed at atmospheric conditions was 0.4 m/s with 20 mPa.s liquid and increased to 0.83 m/s at 20 mbar.
- Another important observation from the data shown in Fig. 6b (taken as Fig. 6a for Plast2 over the low pressure range) is the cross over or "switch" of the constant viscosity data. This leads to a low viscosity fluid entraining air at a speed lower than a high viscosity fluid which is the opposite of what is observed at atmospheric pressure. The switch pressures for 200-100, 100-50 and 50-20 mPa.s are 135, 80 and 30 mbar respectively. The implication in practice is that the "switch" or the steep increase in air entrainment speed with reduced pressure is occurring at lower pressure with high viscosity fluids. In other words, the speed of coating with high viscosity liquids-a desirable

condition- can be increased without going down to a large vacuum. We infer from the data of Fig. 6a that for a 500 mPa.s solution, the switch will occur in the region of 200 mbar, a vacuum not difficult to achieve.

- Experiments below 20 mbars proved very difficult as the air entrainment speed increased sharply and the physical restriction of the rig could not accommodate large reels of substrate. Although, it would be desirable to carry on experiments below 20 mbar to test the extent of the effect of reduced air pressure on air entrainment speeds, the observations below 500 mbars down to 20 mbar are unequivocal: the surrounding hydrodynamic air conditions affect air entrainment and as the pressure is reduced below 50 mbar when the viscosity of the air start to reduce significantly, V_{ae} shoots up, suggesting it will approaches a very high value (infinity?) at zero viscosity. This is the most important result of this study and probably of all experimental studies to date on the fundamental role of the surrounding air viscosity on dynamic wetting.

3.3 Effect of Vacuum Pressures on Rough Substrates

Here we tested three substrates, two of which were paper with increasing roughness and one polyester substrate (Plast1) of roughness similar to the least rough paper. The way in which the dynamic wetting line broke was the same as with the smooth substrates discussed above except that the "v" were smaller and there were many more at comparatively equal viscosities and pressures. As for the air entrainment speed, the results were similar to those obtained with smooth substrates: V_{ae} essentially did not change between 1 bar and 500 mbars but below 500 mbars and more particularly below 50 mbars, further reductions in pressures increased V_{ae} very sharply suggesting again that at zero pressure or zero viscosity V_{ae} would attain a very large value (infinity?). There are however subtle changes in behaviour and it is useful to consider the polyester and paper substrate separately.

Polyester Substrate (Plast1): Both sides of this substrate have marginally different roughness (R_z = 1.92 μm for the front and 1.71 μm for the back) and marginally different initial static contact angle (65^0 for the front and 57^0 for the back) and are expected to display similar V_{ae} at fixed viscosity and pressure. The data in Fig. 7 show that this is the case until we get to a viscosity of 200 mPa.s and a vacuum pressure of 180 mbar when the front and back behaviours diverge significantly with reduced pressure. Specifically, at 200 mPa.s and 80 mbar, the back side of this substrate entrained air at coating speed of 0.33 m/s whereas the front side still coated air free when the coating speed was more than double. Note that all the experiments in our programme were repeated several times, this particular set of experiment was repeated about five times and showed consistently this behaviour. Clearly substrate effects are important- here measured via roughness and initial static contact angle- and a switch has occurred with this substrates at 200 mPa.s and 180 mbars. Similar substrate effects have been reported by Benkreira (2004) at atmospheric pressure, except that here the reduced pressure increases drastically the air entrainment speed. The implication in practice is that when coating high viscosity liquids one may assume we are limited in coating speed. We have shown here, that with the *correct* substrate, a small reduction in operating pressure can lead to high air-free coating speeds. How to define a correct substrate for that purpose, we cannot do at present except to relate it in our case to the measured roughness and initial contact angle (see Table 2). However, given a substrate, we have shown that through experiments, we can obtain a

switch condition. Figure 8 which compares the smooth polyester with the rough polyester illustrates clearly the points made and shows one coating at coating speeds more than twice the other at identical operating conditions. These results are clearly important in practice as they indicate that with moderate decrease in pressure, substrates may "outperform" expectation as viscosity is increased. There may of course be no switch but it is important in practice to test the limits of operation by investigating the "coatability" of a particular substrate at increased viscosity whilst investigating the effect of reduced pressure.

Paper Substrates: The data for these two substrates are now presented and the results are shown in Fig. 9a, b for all viscosities and pressures tested down to the lowest vacuum. The roughness and contact angles of each of the sides of these substrates are given in Table 2. We note, as observed with smooth substrates, that the effect of pressure on V_{ae} become significant only when the pressure is reduced below a low limit, typically less than 100 mbar. Figure 9a displays for each viscosity one pair of lines for roughness front/back 4.40 μm /0.70 μm showing the variation of V_{ae} with pressure. At low viscosity, the smooth side exhibits higher V_{ae} than the rough side. The difference in V_{ae} in each pair reduces as we increase viscosity until we get to a critical viscosity when the pair of lines coincide and both sides exhibit similar V_{ae} at a given pressure. Above the critical viscosity the sides "switch", i.e. the rough side exhibits higher V_{ae} than the smooth side. Such a switch has been observed by Benkreira (2004) for dip coating at atmospheric pressure and the data here at atmospheric pressure confirm the earlier findings that roughness can *increase or decrease* V_{ae} depending on the value of viscosity. The added observation in this data is that the switch, coupled with the increase in V_{ae} with reduced pressure, gives an opportunity to coat high viscosity coatings (high solid content) at much higher speed than expected. For example, at atmospheric pressure, we could coat a 145 mPas solution at speed equivalent to coating an 85 mPa.s solution by changing the roughness from 0.70 μm to 4.40 μm. At pressure of 100 mbar, we can coat the same 145 mPa.s solution at speed equivalent to the 52 mPa.s or less solution by changing the roughness from 0.70 μm to 4.40 μm. Much higher speeds can be attained by lowering the pressure further. This observation is very useful in practice as it implies that if one chooses carefully roughness, one can coat viscous formulation at unexpectedly very high speeds with a moderate vacuum. The data in Fig. 9 b confirms these findings and show that for this particular pair of roughness (1.93 μm/ 3.78 μm), the switch occurs at much lower viscosity 18 mPa.s.

4. CONCLUSIONS

This work has established for the first time the effect of air pressure (viscosity) on air entrainment speeds in coating flows using dip coating as the model flow. Although, experiments could not be realised at the desired 1 mbar values because of the physical dimensions of the vacuum chamber (large reel of substrate are needed because of the high air entrainment speed), the result is unequivocal about the pronounced effect of air pressures when these are reduced below 100 mbars. Air hydrodynamics do have an effect on its entrainment and, with the same coating liquid on the same substrate, more than double the air entrainment speed when the pressure is reduced from atmospheric to 50 mbars. The data presented in this work also confirm the complex

role of roughness, in that it can increase or decrease the air entrainment speed depending on the value on the viscosity of the coating solution. This observation is very useful in practice as it implies that if one chooses carefully roughness one can coat viscous formulation at unexpectedly very high speeds with a moderate vacuum. The observations that V_{ae} is sensitive to both roughness and air pressure (at low pressures) suggest that hydrodynamic effects play a very important role in dynamic wetting- a result we already know when we consider curtain coating (Blake, Clarke and Ruschak, 1994). In these experiments, we "developed" hydrodynamic effects by manipulating the substrate roughness and the conditions of the surrounding air whereas in curtain coating, the effects were developed by manipulating the flow of the liquid on the substrate.

Having now settled the question of the active role of air and hydrodynamics in dynamic wetting, we need to develop further insight of this important effect by measuring Φ, the angle of inclination of the "v" segments, a measure of the maximum speed of wetting and the contact angle θ_D under reduced pressures. Experiments with other gases are also necessary. Such data can then be used to test newly emerging theories on dynamic wetting.

6. ACKNOWLEDGEMENTS

This work was supported by an EPSRC-DTA grant awarded to Mr M.I.Khan whose PhD thesis gives further details on the experimental programme and data. We are grateful for the contribution of Dr Patel to the experimental programme and the support of Ilford Imaging Switzerland Gmbh (Marly) who kindly provided the substrates.

7. NOTATIONS

a_c	Aspect ratio of the dip coater tank
d	substrate-dip coater tank wall distance
H	liquid height in dip coater tank
P	pressure
V	Substrate speed
V*	Maximum speed of wetting
V_{ae}	Air entrainment velocity
R_z	Average peak-to-valley height roughness
T	Temperature
t	time
β	Substrate lateral inclination in angled dip coating
θ_D	Dynamic Contact Angle
Φ	Inclination of the wetting line at $V > V_{ae}$
μ	Viscosity
ρ	Density
σ	Surface tension

8. REFERENCES

Ablett, R. (1923). An investigation of the angle of contact between paraffin wax and water. *Philosphical Magazine* **46**, 244.

Benkreira, H. (2004). The effect of substrate roughness on air entrainment in dip oating. *Chem. Eng. Sci.*, **59**, 2745.

Benkreira, H. and Cohu, O. (1998). Angling the dynamic wetting Line retards air entrainment in pre-metered coating processes. *AIChE J.*, **4**, 1207.

Blake, T.D. (1993). Dynamic Contact Angles and Wetting Kinetics. In Wettability, ed. J. Berg, Chap. 5, p.252. Marcel Dekker, New-York, U.S.A.

Blake, T.D. and Haynes, J.M. (1969). Kinetics of liquid/liquid displacement. Journal of *Colloid and Interface Science J.*, **30**, 421.

Blake, T.D., Clarke, A. and Ruschak, K.J.(1994). Hydrodynamic assist of dynamic wetting. *AIChE J.*, **40**, 229.

Blake, T.D. and Ruschak, K.J. (1979). A maximum speed of wetting. *Nature*, **282**, 489

Blake, T.D. and Shikhmurzaev, Y.D. (2002). Dynamic wetting by liquids of different viscosity. *Colloid and Interface Science J.*, **253**, 196.

Buonoplane, R.A., Gutoff, E.B. and Rimore, M.M.T. (1986). Effect of Plunging Tape Surface Properties on Air Entrainment Velocity. *AIChE J.*, **32**, 682.

Burley, R. and Jolly, R.P.S. (1984). Entrainment of Air into Liquids by a High Speed Continuous Solid Surface. *Chem. Eng. Sci.*, **39**, 1357.

Burley, R. and Kennedy, B.S. (1976). An experimental study of air entrainment at a solid-liquid-gas interface. *Chem. Eng. Sci.*, **31**, 901

Burley, R. (1992). Air entrainment and the limit of coatability. *Journal of the Oil and Colour Chemists Association*, **75**, 192.

Cohu, C. and H. Benkreira, H. (1998). Air Entrainment in angled dip coating. *Chem. Eng. Sci.*, **53**, 533.

Cohu, C. and H. Benkreira, H. (1998). Entrainment of air by a solid surface plunging into a non-Newtonian liquid. *AIChE J.*, **44**, 2360.

Cox, R.G. (1986). The dynamics of the spreading of liquids on a solid surface. Part 1. Viscous flow. *J. Fluid Mech.*, **168**, 169.

Deryagin, B.M., and Levi, S.M. (1964). Film Coating Theory, p.137. Focal Press, London, U.K.

Gutoff, E.B. and Kendrick, C.E. (1982). Dynamic Contact Angles. *AIChE J.*, **28**, 459.

Khan, M.I. (2006). Dynamic Wetting under vacuum and with rough substrates. Ph.D. Thesis, University of Bradford, UK.

Miyamoto, K. (1991). On the mechanism of air entrainment. *Industrial Coating Research*, **1**, 71.

O'Connell, A. (1989). Observation of air entrainment and the limits of coatability. Ph.D. Thesis, Heriot-Watt University, Edinburgh, Scotland.

Scriven, L.E. (1982). How does air entrain at wetting lines? *AIChE* Winter National Meeting, Orlando, USA.

Shikhmurzaev, Y.D. (1993). The moving contact line on a smooth solid surface. *Int. J. Multiphase Flow*, **19**, 589

Shikhmurzaev, Y.D. (1997). Moving contact lines in liquid / liquid / solid systems. *Journal of Fluid Mechanics*, **334**, 211.

Severtson, Y.C. and Aidun, C.K. (1996). Stability of two-layer stratified flow in inclined channels: applications to air entrainment in coating systems, *Journal of Fluid Mechanic*, **312**, 173.

Teletzke, G.F., Davis, H.T. and Scriven, L.E. (1988). Wetting hydrodynamics. *Rev. Phys. Appl.*, **23**, 989.

Wilkinson, W.L. (1975). Entrainment of air by a solid surface entering a liquid/air interface. *Chem. Eng. Sci.*, **30**, 1227.

LIST AND CAPTIONS OF TABLES AND FIGURE

LIST AND CAPTIONS OF TABLES

Table 1: Measured physical properties of coating fluids used: silicone oils (1-6) at 25 °C and glycerine-water solutions (7-15) at 26.5 °C.

Table 2: Roughness of the substrates used and corresponding contact angles with silicone oil sample 3 in Table 1 of viscosity approximately 50 mPa.s.

Table 1: Measured physical properties of coating fluids used: silicone oils (1-6) at 25 °C and glycerine-water solutions (7-15) at 26.5 °C.

Coating Fluids	Viscosity (mPa.s)	Surface Tension (mN/m)	Density (kg/m^3)
1	9	19	900
2	18	19	930
3	50	19	951
4	87	20	958
5	181	19	962
6	459	19	963
7	40	66	1203
8	84	65	1221
9	140	64	1231
10	192	65	1237
11	259	64	1243
12	368	63	1248
13	493	63	1251
14	604	63	1254
15	733	64	1256

Table 2: Roughness of the substrates used and corresponding contact angles with silicone oil sample 3 of viscosity approximately 50 mPa.s.

Substrate	**R_a (μm)**	**$R_y = R_z$ (μm)**	**$\theta_{t = 0s}$**	**$\theta_{t = 3s}$**
10908F (Pap1F)	0.73	4.40	78.40	11.97
10908B (Pap1B)	0.10	0.70	57.28	5.65
10929F (Pap2F)	0.63	3.78	63.31	12.90
10929B (Pap2B)	0.32	1.93	56.76	8.40
NSFM F (Plast1F)	0.31	1.92	64.78	12.99
NSFM B (Plast1B)	0.28	1.71	56.97	13.39
53818F (Plast2F)	0.05	0.30	56.50	12.38
53818B (Plast2B)	0.03	0.19	60.18	12.18
53281F (Plast3F)	0.03	0.30	59.60	13.71
53281B (Plast3B)	0.07	0.21	56.71	10.95

LIST AND CAPTIONS OF FIGURES

Figure 1: Dynamic wetting in dip coating: contact angle, "vvv" line and maxiumum speed of wetting.

Figure 2: Experimental set-up showing a dip coater housed within a vacuum chamber.

Figure 3: Contact angle evolution in time for the substrates-coating solutions system: **(a)** Silicone (50 mPa.s) over time 0-1 s, **(b)** Silicone (50 mPa.s) over time 1-7 s, **(c)** Glycerol (50 mPa.s) over time 0-5 s and **(d)** Glycerol (50 mPa.s) over time 0-30 s.

Figure 4: Validation of the experimental technique against previous air entrainment speed data at atmospheric pressure.

Figure 5: The formation of 1 large "v" with the smooth polyester substrate Plast2 with the glycerine solution of viscosity 40 mPa.s at atmospheric pressure. The substrate delimited by the two white lines is looked from an angle. The dark "V" observed is about 5 cm in height.

Figure 6a: Air entrainment speeds measured at reduced pressures with smooth polyester substrates Plast2 and Plast3.

Figure 6b: Cross over or "switch" of the constant viscosity data of Plast 2 observed in the low pressure range.

Figure 7: Air entrainment speeds measured at reduced pressures with the marginally rough polyester substrate Plast1.

Figure 8: Comparative performance of the smooth (Plast2) and marginally rough polyester (Plast1) substrates.

Figure 9a, b : Air entrainment speeds measured at reduced pressures with Pap1 and Pap2.

Figure 1: Dynamic wetting in dip coating: side and front view showing contact angle, "vvv" line and maxiumum speed of wetting.

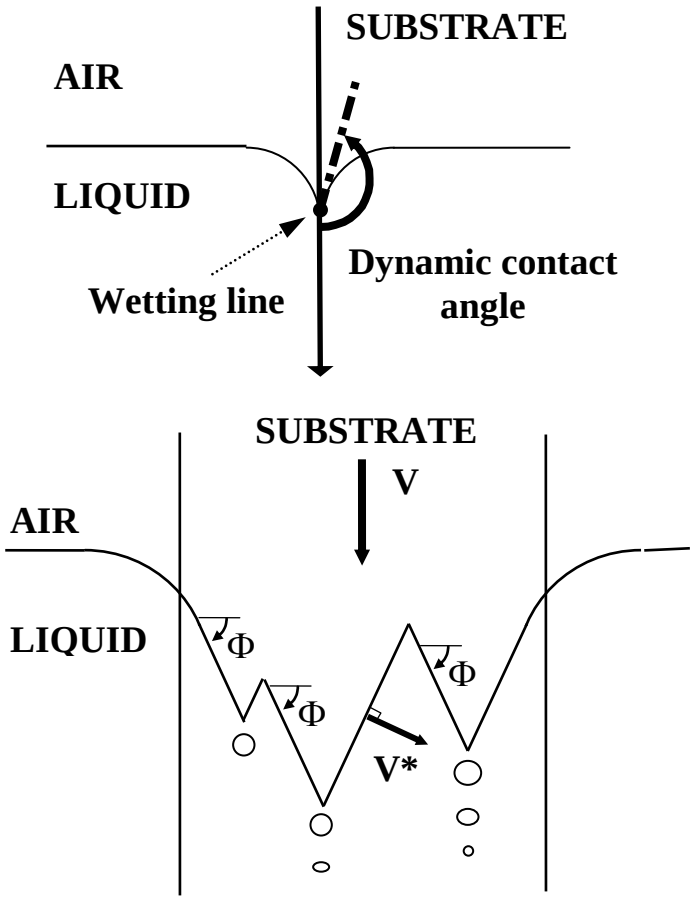

Figure 2: Experimental set-up showing a dip coater (see Khan, 2006) housed within a vacuum chamber.

Figure 3a: Contact angle evolution in time for the substrates-coating solutions system: **(a)** Silicone (50 mPa.s) over time 0-1 s, **(b)** Silicone (50 mPa.s) over time 1-7 s, **(c)** Glycerol (50 mPa.s) over time 0-5 s and **(d)** Glycerol (50 mPa.s) over time 0-30 s.

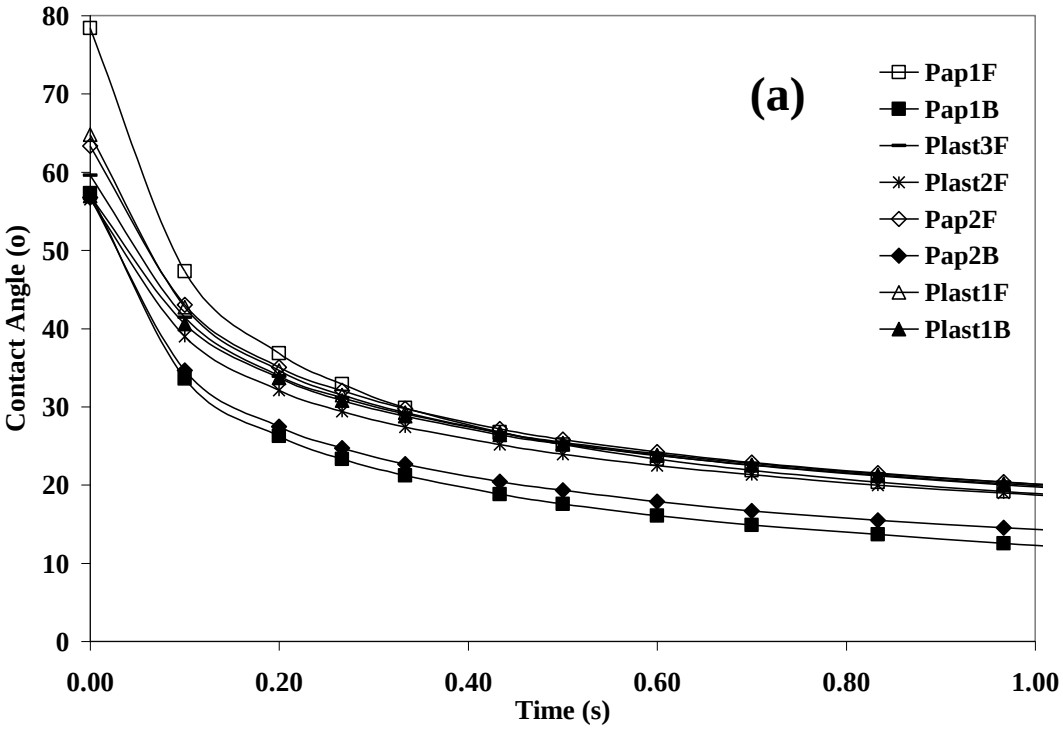

Figure 3b: Contact angle evolution in time for the substrates-coating solutions system: Silicone (50 mPa.s) over time 1-7 s.

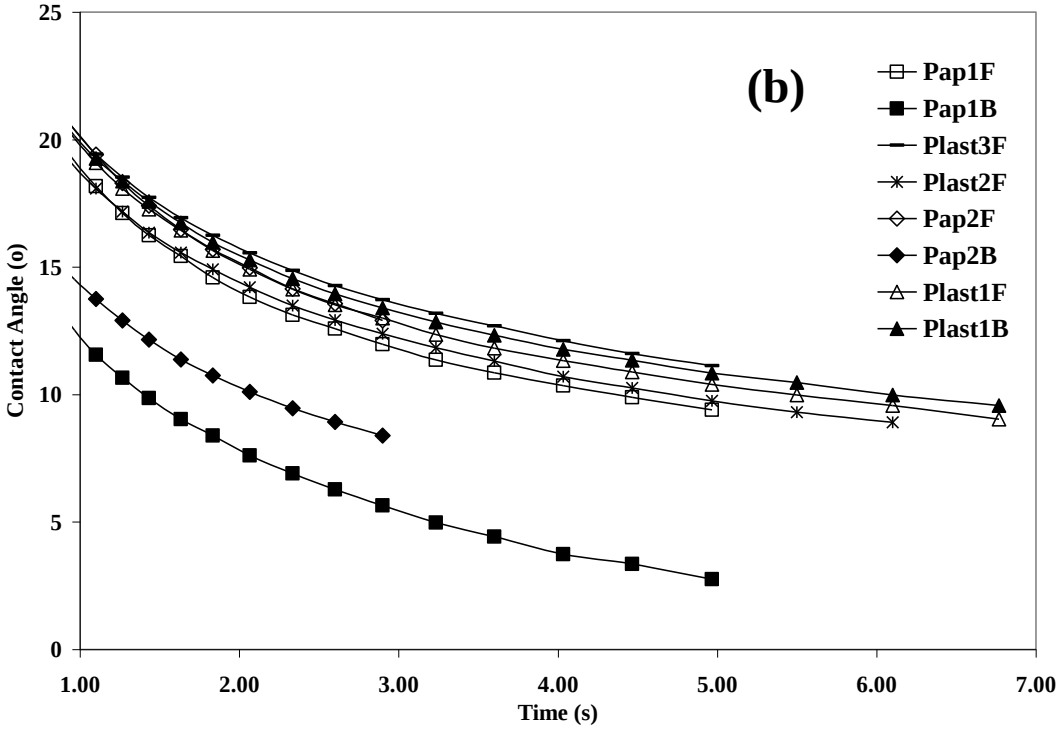

Figure 3c: Contact angle evolution in time for the substrates-coating solutions system: Glycerol (50 mPa.s) over time 0-5 s

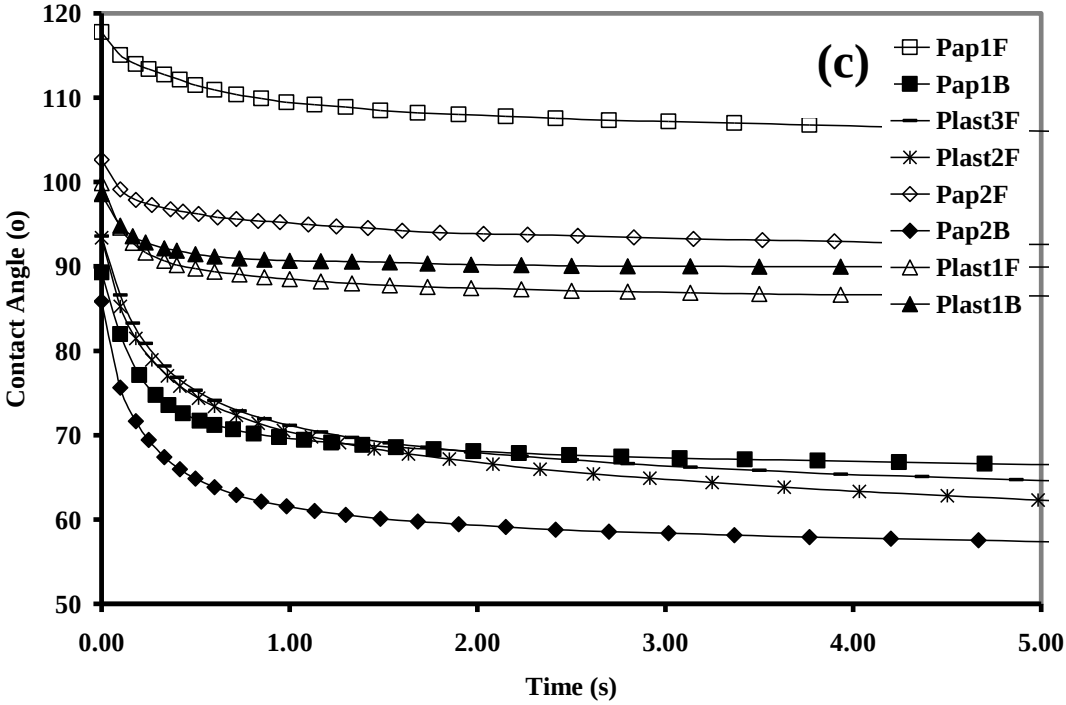

Figure 3d: Contact angle evolution in time for the substrates-coating solutions system: Glycerol (50 mPa.s) over time 0-30 s.

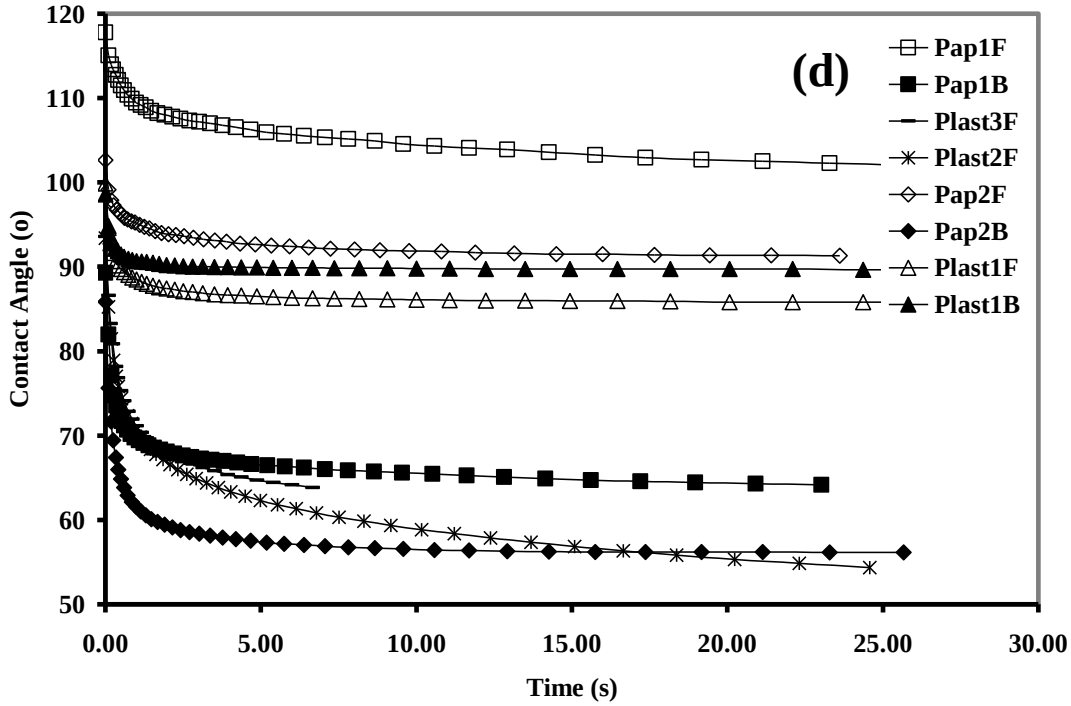

Figure 4: Validation of the experimental technique against previous air entrainment speed data at atmospheric pressure. Note how the silicone data (trend line linking them) deviates highlighting the importance of surface tension.

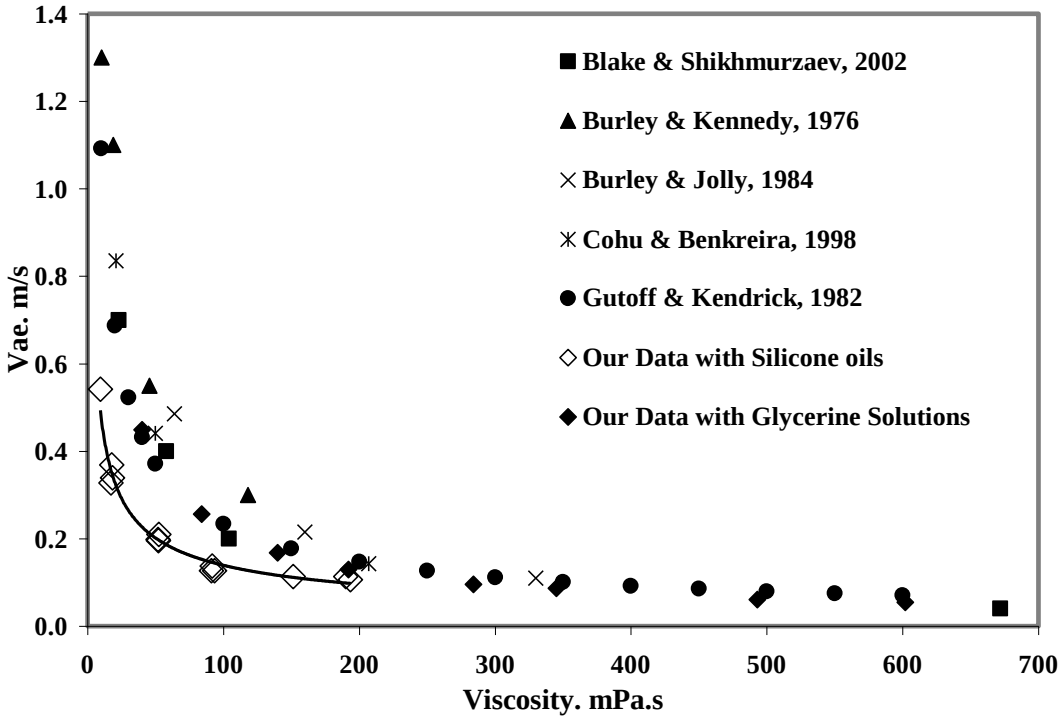

Figure 5: The formation of 1 large “v” with the smooth polyester substrate Plast2 with the glycerol solution of viscosity 40 mPa.s at atmospheric pressure. The substrate delimited by the two white lines is looked from an angle. The dark “V” is about 5cm in height.

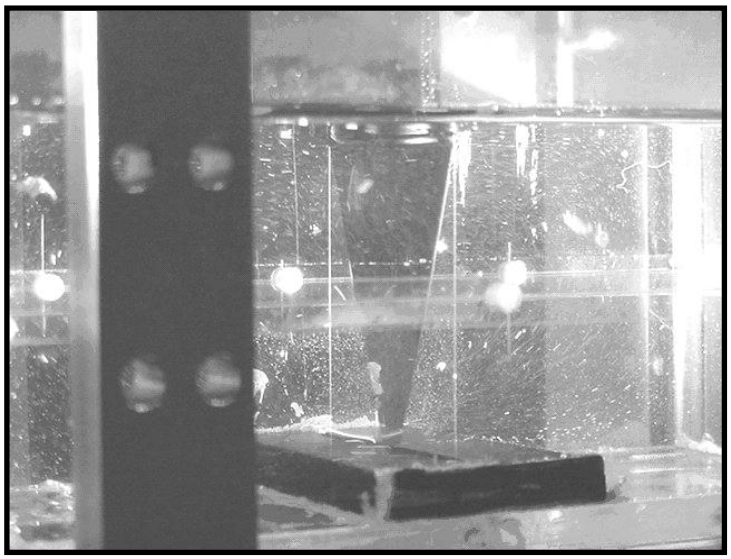

Figure 6a: Air entrainment speeds measured at reduced pressures with smooth polyester substrates Plast2 and Plast3F (one data point at 100 mPa.s).

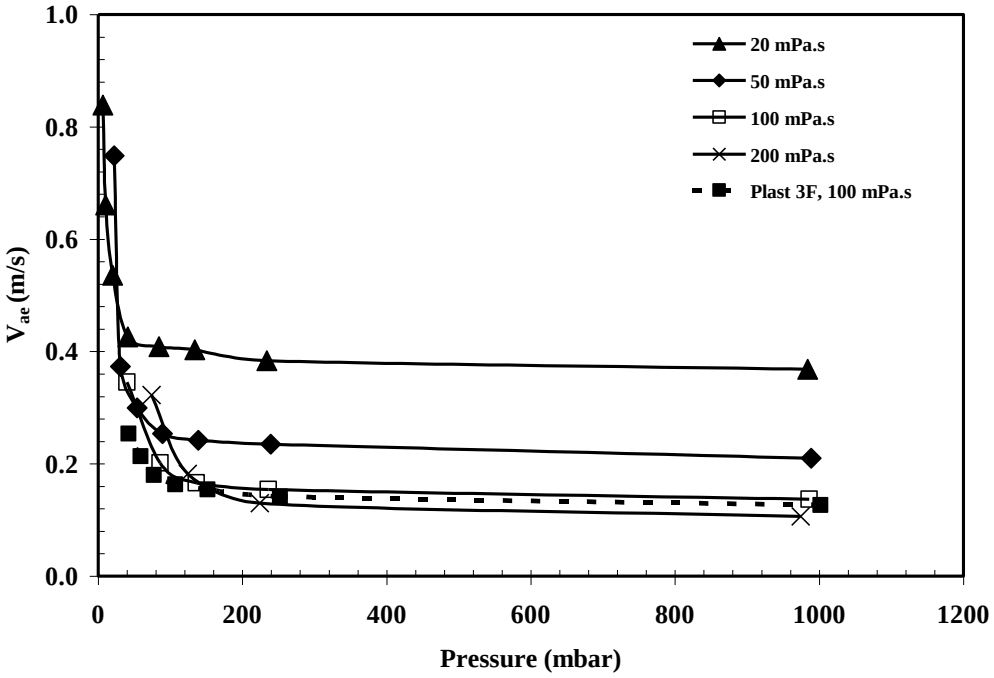

Figure 6b: Cross over or "switch" of the constant viscosity data of Plast2 observed in the low pressure range.

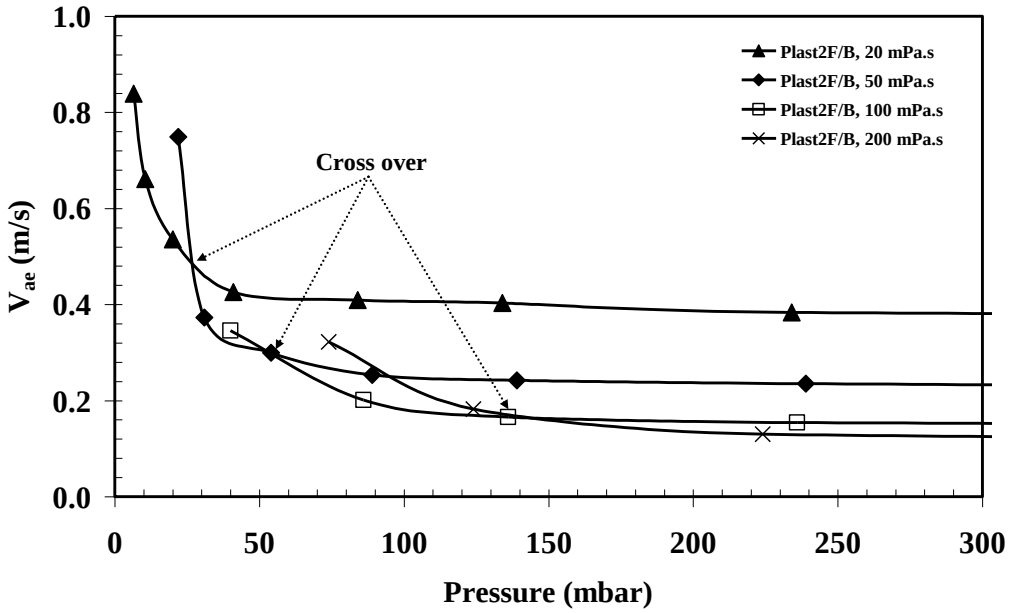

Figure 7: Air entrainment speeds measured at reduced pressures with the marginally rough polyester substrate Plast1.

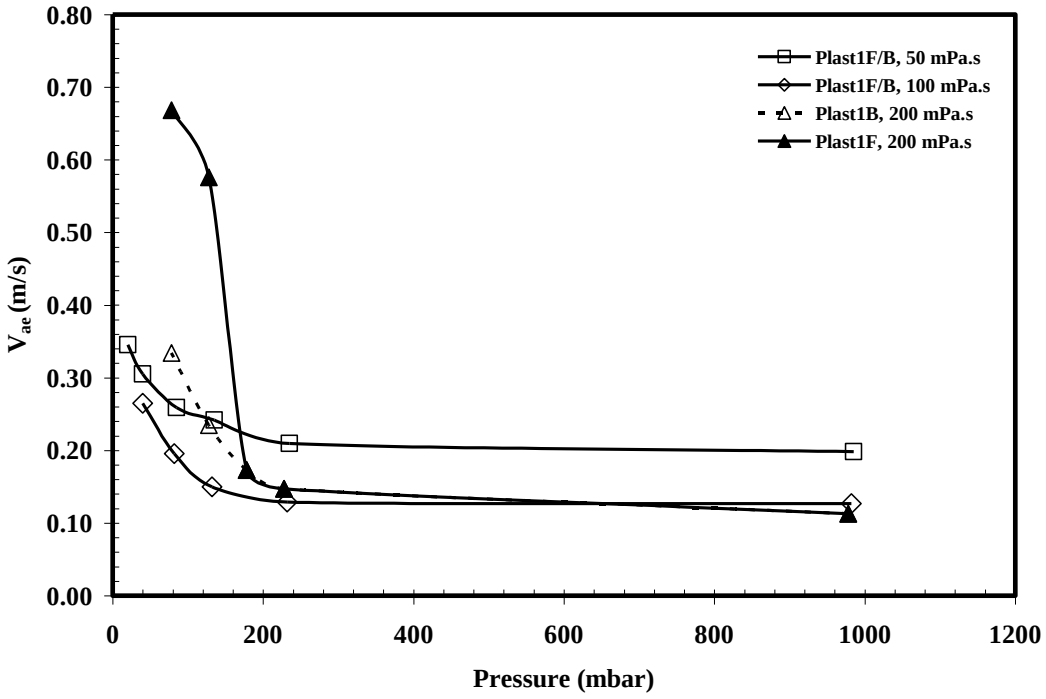

Figure 8: Comparative performance of the smooth (Plast2) and marginally rough polyester (Plast1) substrates.

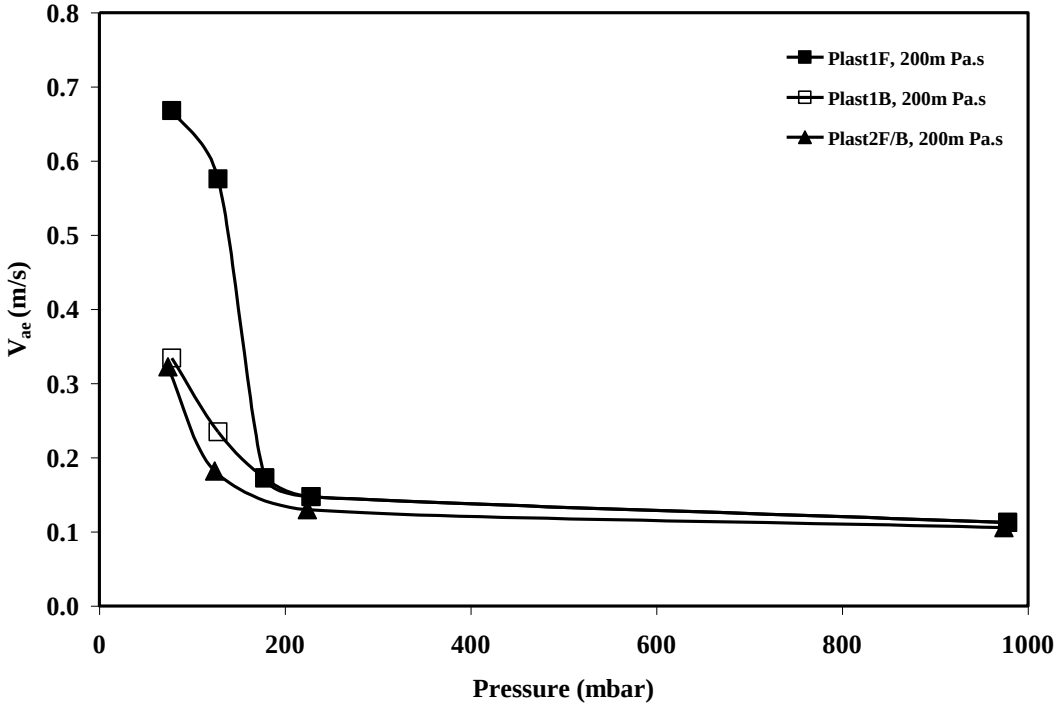

Figure 9a: Air entrainment speeds measured at reduced pressures with Pap1 and Pap2.

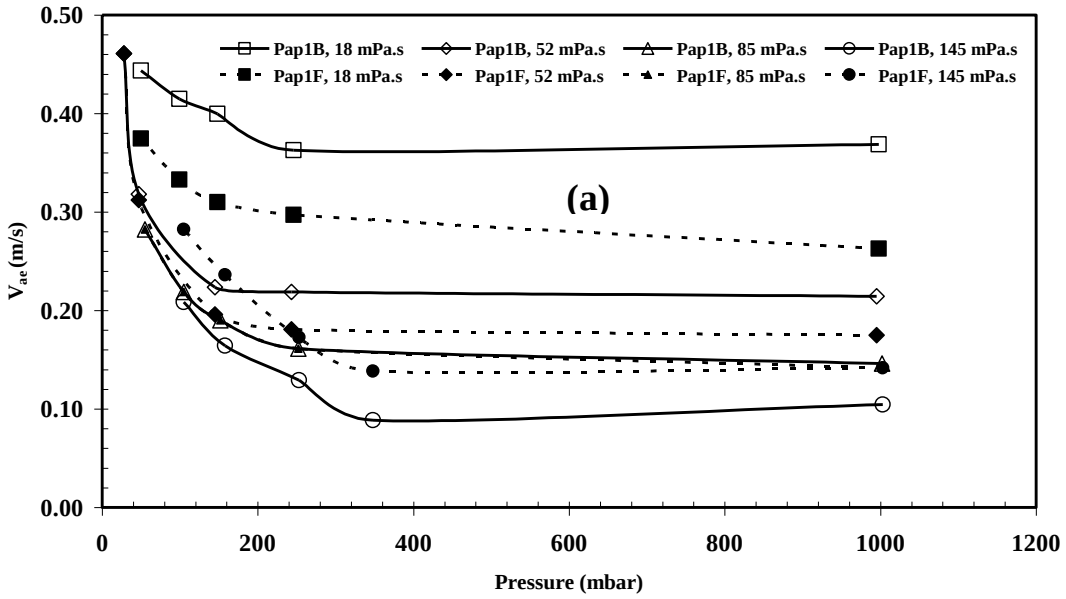

Figure 9b: Air entrainment speeds measured at reduced pressures with Pap1 and Pap2.